

Removal of aniline from aqueous solutions by activated carbon coated by chitosan

Qian Liu, Lujie Zhang, Pan Hu and Ruihua Huang

ABSTRACT

In this work, activated carbon (AC) coated by chitosan was synthesized and characterized by Fourier transform infrared spectrophotometer and scanning electron microscope (SEM) techniques. The removal of aniline from aqueous solutions by AC coated by chitosan was investigated. The factors affecting the adsorption of aniline onto AC coated by chitosan, including the ratio of AC to chitosan, adsorbent dosage, pH value of solution, initial aniline concentration, and contact time were evaluated. These results showed that the optimum operating conditions were: the ratio of AC to chitosan = 0.5, adsorbent dosage = 0.2 g, and the adsorption of aniline from aqueous solutions had better removal in the concentration range of 20–50 mg/L. This adsorbent allowed high removal toward aniline in a wide range of pH. The equilibrium time was 100 minutes. The Freundlich model exhibited better correlation of the equilibrium adsorption data. The pseudo-second-order kinetic equation could better describe the kinetic behavior of aniline adsorption.

Key words | activated carbon coated by chitosan, adsorption, aniline, isotherms

Qian Liu
Lujie Zhang
Pan Hu
Ruihua Huang (corresponding author)
College of Science,
Northwest A&F University,
Yangling, Shaanxi 712100,
China
E-mail: hrh20022002@163.com

INTRODUCTION

Aniline is frequently used as a raw material by the chemical industry, i.e. in the manufacture of dyes, rubbers, pharmaceutical preparation, plastic and paint. It is also a common byproduct of the paper and textile industries. It is known to be a toxic pollutant and its presence in wastewater, even in very low concentrations, has been shown to be harmful to aquatic life (An *et al.* 2009). Traditionally, aniline-containing wastewater was treated using photodecomposition (Chu *et al.* 2007), electrolysis (Han *et al.* 2006), adsorption (Al-Johani & Salam 2011), oxidation (Sapurina & Stejskal 2012) and biodegradation (Wang *et al.* 2011). Among these methods, adsorption has been shown to be the most promising option for the removal of organic contaminants from wastewater in the case of low concentrations, due to the low cost and high efficiency (Hu *et al.* 2013; Yakout *et al.* 2013). Activated carbon (AC) has been considered as a popular adsorbent due to its high adsorption capacity, high adsorption rate and good resistance to abrasion. However, the lack of dispersion of

AC powder brings into question its further application (Xu *et al.* 2015). To pave the way for the application of AC in the treatment of wastewater, many efforts have been made to maintain the high adsorption capacity of AC and reduce the cost of AC. The coating of AC with biological materials, such as chitosan and cellulose, is a new method for its modification. By this modification, much lower quantities of AC will be needed in the adsorption process and the removal process becomes cost-effective. Chitosan is a biopolymer with a linear polysaccharide based on glucosamine units, which may be obtained by the deacetylation of chitin (a natural polymer). Meanwhile, chitosan is an environmentally friendly material due to these advantages, including its abundance, non-toxicity, biocompatibility and biodegradability. It has been applied in many fields including food processing, agriculture, medicine, textiles, and wastewater treatment, etc. At present, chitosan and its derivatives, such as cross-linked chitosan, chitosan beads and chitosan composite, have been studied as adsorbents

for the removal of organic pollutants and dyes from aqueous solutions (Gupta *et al.* 2012; Liu *et al.* 2012; Xie *et al.* 2012).

In this study, AC coated by chitosan was synthesized and characterized, and the adsorption capacity of AC coated by chitosan for aniline was investigated. The effects of the ratio of AC to chitosan, adsorbent dosage, the initial pH value of the aniline solution and contact time on the adsorption of aniline onto AC coated by chitosan were determined. Further, the experimental adsorption data were analyzed by different kinetic and isotherm models (see Supporting information, available in the online version of this paper).

MATERIALS AND METHODS

Materials

Chitosan powder (90% deacetylated) was acquired from the Sinopharm Group Chemical Reagent Limited Company (China). The AC powder was used without further purification. All other reagents used, including acetic acid, sulfuric acid, hydrochloric acid, and sodium hydroxide, were of analytical grade. A stock aniline solution of 1,000 mg/L was prepared by dissolving 1 g of aniline (Tianjin Bodi Chemical Co., Ltd, purity = 99.5%) in 1 L of deionized water. The pH values of aniline solutions were adjusted by adding 0.1 mol/L hydrochloric acid or 0.1 mol/L sodium hydroxide solutions.

Preparation of activated carbon coated by chitosan

AC coated by chitosan was prepared according to the literature (Hydari *et al.* 2012) with some modifications. Five grams of AC was poured into 2 mol/L of sulfuric acid for 4 hours. The AC was washed with deionized water after filtration and dried in an oven at 60 °C. The chitosan powder was dissolved into 2% (v/v) acetic acid, thereby obtaining a 2 wt % solution. Acid treated AC was added slowly into this solution, the ratio of AC to chitosan being 0.5. After the mixed solution was stirred for 40 minutes, it was coated in culture vessels and then dried at 60 °C to form membranes. Subsequently, these membranes were soaked in 0.1 mol/L sodium hydroxide solution to separate them from the culture

dishes. The membranes were washed with distilled water to neutral pH and dried at 60 °C. Finally, these dry membranes were ground and sieved to obtain 100-mesh size particles, which were then applied in the adsorption studies.

Instrumentation

The aniline concentration was determined by a double beam UV-vis spectrophotometer (Unicam UV-2, China) at 545 nm by naphthyl ethylenediamine azo photometry. Other instruments included a circulating water pump (Zhengzhou Dufu Instrument Co., Ltd, China, SHB-3), a thermostated shaker (Jintan Kanghua Electronic Instrument Co., Ltd, China, SHA-B), a cantilever constant speed mixer (Jintan Kanghua Electronic Instrument Co., Ltd, China, JJ-1B) and a pH meter (Shanghai LiDa Co., Ltd, China). The surface morphology of AC and AC coated by chitosan was determined by a field emission scanning electronic microscope (FE-SEM) (Hitachi S4800). The Fourier transform infrared spectroscopy (FTIR) spectra of AC, chitosan and AC coated by chitosan were determined by the FTIR. Spectra were collected with a spectrometer using potassium bromide pellets. In each case, 1 mg of dried sample and 100 mg of potassium bromide were homogenized using a pestle and mortar, and pressed into a transparent tablet. The pellets were analyzed with a FTIR spectrometer (Shimadzu 4100) in the transmittance (%) mode with a scan resolution of 4 cm⁻¹ in the range 4000–400 cm⁻¹.

Adsorption experiments

Adsorption experiments were conducted by changing the ratio of AC to chitosan, adsorbent dosage, the initial aniline concentrations, the pH values of aniline solutions, and the contact time. The pH values of the aniline solutions were adjusted to a given value by adding either 0.1 mol/L hydrochloric acid or sodium hydroxide solutions before the adsorption experiments were performed. In all adsorption experiments, a certain amount of adsorbent was placed in a 100 mL Erlenmeyer flask, into which 50 mL of aniline solution was added. These flasks were agitated on a thermostated shaker at 200 rpm. When the defined time was attained, the supernatant was filtered through filter paper to determine the residual concentrations. The

adsorption capacity at any time t (q_t , mg/g) was calculated according to Equation (1):

$$q_t = \frac{(C_0 - C_t)V}{W} \quad (1)$$

where C_0 and C_t are the concentrations of aniline in aqueous solution at the initial time and at any time t , respectively (mg/L); V is the volume of aniline solution (L); and W is the mass of adsorbent (g). The removal toward aniline (R) was calculated using the following equation:

$$R = \frac{C_0 - C_t}{C_0} \times 100 \quad (2)$$

Desorption study

To better understand the mechanism of aniline adsorption onto the adsorbent, desorption experiments were conducted. After performing the equilibrium study with different initial aniline concentrations ranging from 20 to 250 mg/L, aniline-adsorbed particles were collected by

filtration and then dried at room temperature. Fifty mL of ethanol and acetone solutions were used for the regeneration of AC coated by chitosan. These solutions were stirred for 6 hours at 200 rpm and 20 °C. The particles were removed and rinsed with distilled water and then reused for the adsorption of aniline solutions.

RESULTS AND DISCUSSION

Characteristics of AC coated by chitosan

Figure 1 shows the SEM micrographs of AC and AC coated by chitosan under different magnifications (1000 (Figure 1(a) and 1(a')) and 3000 (Figure 1(b) and 1(b')). From Figure 1, it was found that AC coated by chitosan had a more developed honeycomb structure compared to raw AC. Besides, AC coated by chitosan becomes rigid relative to raw chitosan. The rigidity would endow this adsorbent with good settlement properties. During the adsorption experiments, we observed that this adsorbent settles rapidly.

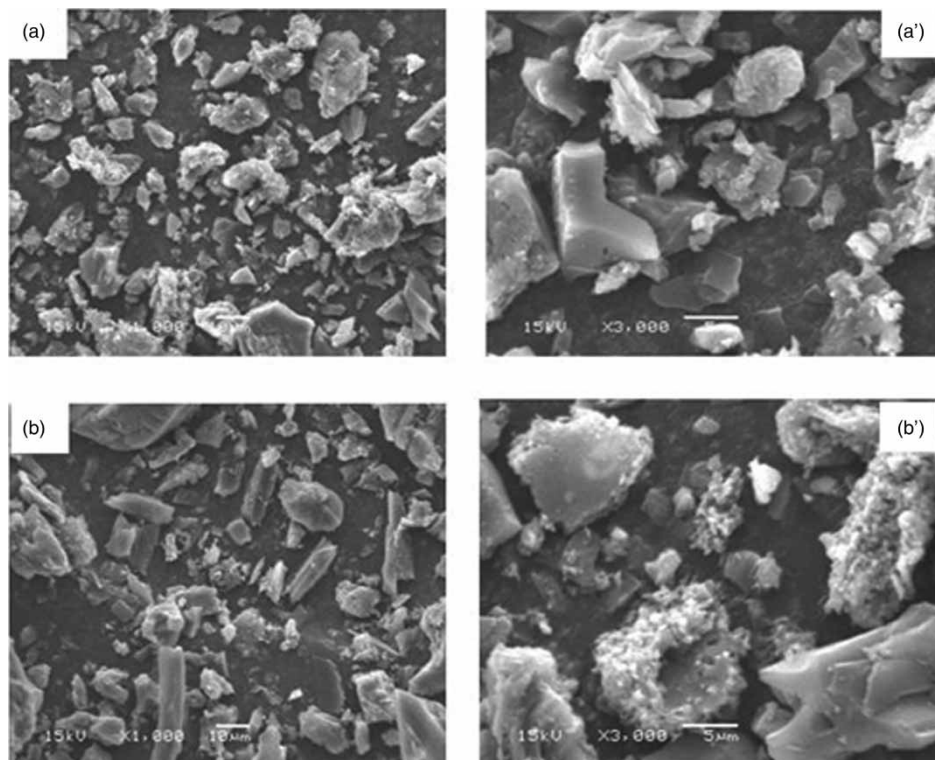


Figure 1 | SEM images of AC (a, a') and AC coated by chitosan composite (b, b').

The FTIR spectrum is a useful tool to identify functional groups in a molecule, as each specific chemical bond often has a unique energy absorption band. The FTIR spectra of chitosan, AC and AC coated by chitosan were obtained using an FTIR spectrometer (Avatar-360, Nicolet) to confirm the presence of functional groups, as shown in Figure 2. In the FTIR spectra for chitosan, the adsorption band around 3443 cm^{-1} can be attributed to the stretching vibration of O-H, the extension vibration of N-H bonds, and the adsorption band at 1658 cm^{-1} can be attributed to the N-H bending vibration of NH_2 groups in chitosan. The peak corresponding to the $-\text{NH}$ deformation vibration in $-\text{NH}_2$ was observed at 1380 cm^{-1} . In the FTIR spectra of AC, the peaks at 2987 , 2855 , 1641 and 1428 cm^{-1} present C-H aliphatic stretching, $-\text{O}-\text{CH}_3$ of aldehyde group, stretching vibrations of $\text{C}=\text{O}$ in carbonyl, lactonic and carboxyl groups and stretching of C-O or O-H deformation in carboxylic acids, respectively (Hydari *et al.* 2012). In the FTIR spectra of AC coated by chitosan, these peaks at 3442 , 1658 and 1380 cm^{-1} are associated with the characteristic peaks of chitosan that appeared (Liu & Zhang 2015). However, their intensities decreased obviously, indicating that contact between the AC and chitosan had occurred.

Effect of the ratio of activated carbon to chitosan

To investigate the effect of the ratio of AC to chitosan on aniline adsorption, a series of AC coated by chitosan was prepared by changing the ratio of AC to chitosan. The results are shown in Figure 3. Chitosan alone had almost no removal toward aniline, while AC alone showed high removal. AC coated by chitosan showed increasing removal, with the ratio of AC to chitosan being from 0.25 to 0.5.

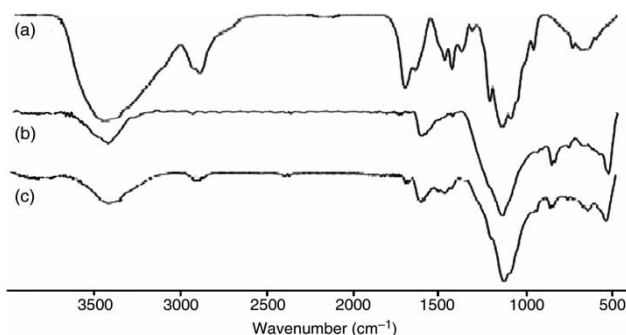


Figure 2 | FTIR spectra of chitosan (a), AC (b) and AC coated by chitosan (c).

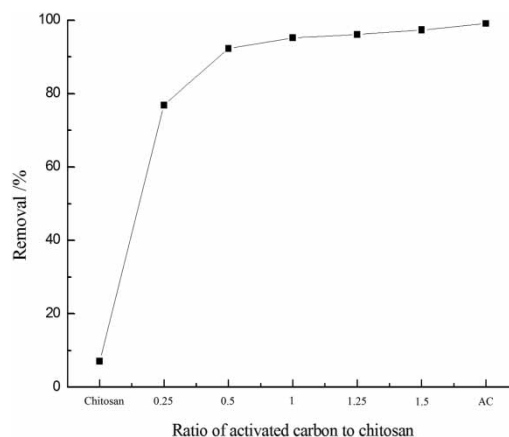


Figure 3 | Effect of the ratio of AC to chitosan on aniline adsorption.

When this ratio was higher than 0.5, high and stable removal (close to that of AC powder alone) toward aniline was observed. An increase in this ratio indicated an increase in AC content in this composite. As we know, AC was often applied in the adsorption of many pollutants, especially organic pollutants (Ma *et al.* 2013). However, it was difficult to realize the separation of solids and liquids by filtration. In this experiment, AC coated by chitosan allowed relatively good settleability due to the introduction of chitosan, as compared with AC. Considering the removal toward aniline together with the compatibility between AC and chitosan, the ratio of AC to chitosan was fixed at 0.5 in this composite.

Effect of adsorbent dosage

To investigate the effect of adsorbent dosage on aniline adsorption, these experiments were carried out with initial aniline concentrations of 20 mg/L at 20°C and 200 rpm . As shown in Figure 4, the removal increased with increasing adsorbent dosage due to the increase in the total available surface area of the adsorbent particles (Xiong *et al.* 2011). The removal toward aniline reaches up to 93.0% for 0.2 g of adsorbent dosage. When the adsorbent dosage exceeded 0.2 g , the removal toward aniline increased slowly. However, the adsorption capacity decreased with an increase in adsorbent dosage. This decrease in adsorption capacity may be attributed to overlapping or aggregation of adsorption sites resulting in a decrease in total adsorbent surface area available for aniline and an increase in diffusion path length (Crini & Badot 2008). Considering the removal as

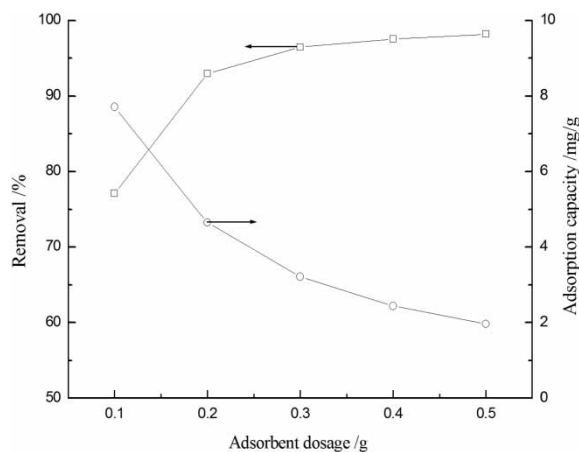


Figure 4 | Effect of adsorbent dosage on aniline adsorption.

well as the adsorption capacity, 0.2 g of adsorbent dosage was chosen for further experiments.

Effect of initial aniline concentration

Figure 5 shows the variation of removal toward aniline with respect to the initial aniline concentrations at natural pH and 20 °C. The removal decreased with an increase in initial aniline concentration at a fixed adsorbent dosage (0.2 g). This trend may be explained as follows: at lower concentrations, the ratio of the initial number of aniline molecules to the available adsorption sites was low and subsequently more adsorption sites were available for aniline molecules, thus the removal increased. However, at higher concentrations,

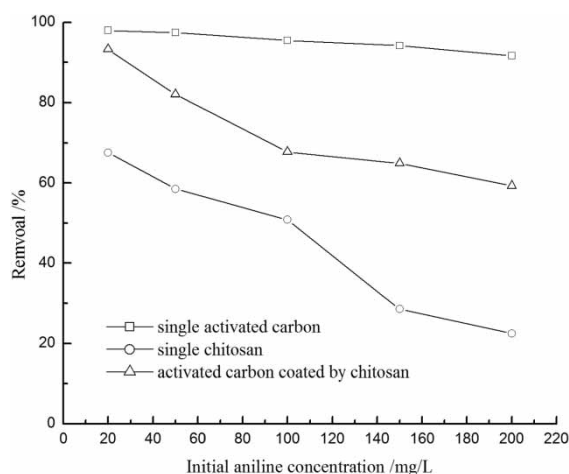


Figure 5 | Effect of initial aniline concentration on aniline adsorption.

the ratio of the initial number of available adsorption sites to aniline molecules was low, the number of available adsorption sites became lower and thus the removal toward aniline reduced (Viswanathan *et al.* 2009). As shown in Figure 3, chitosan alone had low removal toward aniline while AC alone showed high removal toward aniline. Considering the cost of the experiment, AC coated by chitosan was likely to be a good adsorbent for the removal of aniline from aqueous solutions in the concentration range of 20–50 mg/L when the adsorbent dosage was 0.2 g.

Effect of pH value of aniline solutions

It is well known that the initial pH value of a system is an important parameter in the adsorption of adsorbate. In this study, the adsorption of aniline onto AC coated by chitosan was studied at six different initial pH levels by maintaining 180 minutes as the contact time, 0.2 g as adsorbent dosage, using 20 and 50 mg/L initial aniline concentration at 20 °C. Figure 6 shows the removal as a function of pH value of the solutions. The pK_a value of aniline at 20 °C is approximately 4.6 (Chang *et al.* 2012). When the pH value of the solution exceeds the pK_a of aniline, aniline molecules exist in the solution. When the pH value of the solution is lower than 4.6, aniline molecules are ionized to the positively charged anilinium ions. At low pH values, aniline existed in the form of anilinium ions, and a part of the $-NH_2$ groups in chitosan was protonated into $-NH_3^+$, thus it was difficult for the

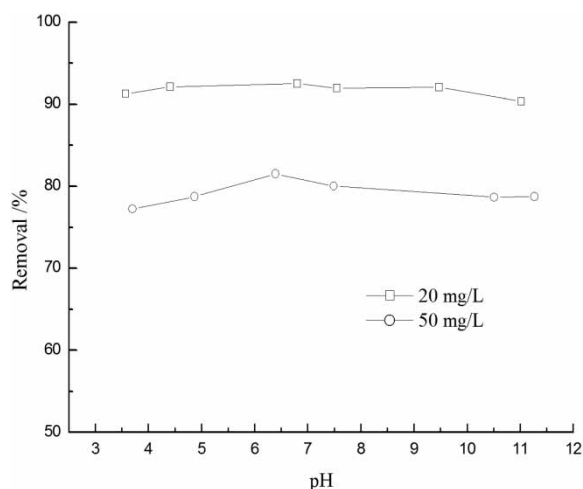


Figure 6 | Effect of pH value on aniline adsorption.

anilinium ions to approach the AC due to the repulsive interaction between the $-\text{NH}_3^+$ and anilinium ions, leading to low removal toward aniline. However, at high pH values (>6), high removal toward aniline may be attributed to the fact that aniline molecules were prone to be adsorbed onto AC by the Van der Waals force. Besides, from these results shown in Figure 6, this adsorbent could remove aniline in a relatively wide range of pH values. Because this adsorbent gave relatively high removal toward aniline at natural pH value, the pH value of the aniline solution was not adjusted for further adsorption experiments.

Effect of particle size

Figure 7 illustrates the removals toward aniline as a function of a particle size of 35-mesh, 100-mesh and 200-mesh in the range of initial aniline concentrations of 20–200 mg/L at 20 °C. As can be seen in Figure 7, the removal adsorbed by AC coated by chitosan corresponded to an increasing trend: 200-mesh $>$ 100-mesh $>$ 35-mesh. The increase in aniline adsorption with the adsorbent particle size was attributed to the increase in surface area of the adsorbent and the increase in availability of vacant adsorption sites.

Effect of contact time

Figure 8 illustrates the removals toward aniline as a function of contact time in the range of 5–180 minutes at 20 °C. The

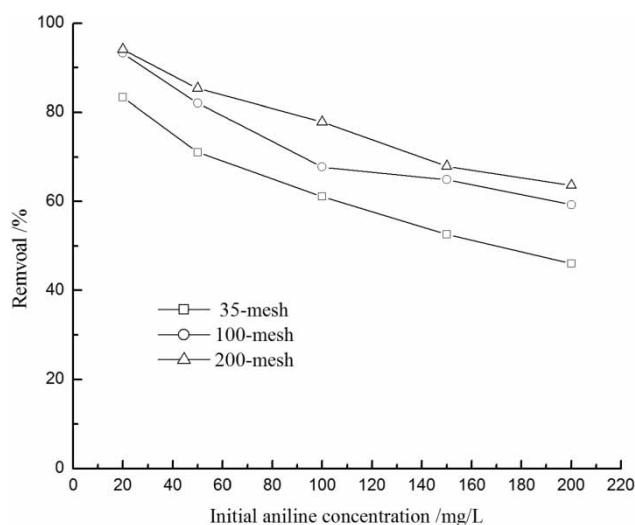


Figure 7 | Effect of particle size on aniline adsorption.

rate of aniline adsorption was initially rapid and then slowed down gradually until equilibrium was reached, beyond which there was no further adsorption. The rapid adsorption at the initial stage can be attributed to the availability of a large number of vacant sites for the adsorption of aniline, and the slow rate of aniline adsorption was probably due to the slow pore diffusion of the adsorbate into the bulk of the adsorbent. Besides, as shown in Figure 8, a shorter equilibrium time was required with increasing initial aniline concentrations, and the time needed for aniline solutions at 20 mg/L, 50 mg/L, and 100 mg/L to reach equilibrium was 100, 40, and 20 minutes, respectively. For the sake of the attainment of equilibrium, an equilibrium time of 100 minutes was considered to be optimum in the isotherm experiments.

To examine the controlling mechanism of the adsorption process further, the pseudo-second-order adsorption kinetic model (Chandra *et al.* 2010) was used to test the experimental data for adsorption of aniline on the particles:

$$\frac{t}{q_t} = \frac{1}{k_2 q_e^2} + \frac{1}{q_e} t \quad (3)$$

where q_e and q_t are the amounts of aniline adsorbed (mg/g) at equilibrium and at any time, t (min), respectively. The values of q_e and the adsorption rate constant k_2 can be obtained by plotting t/q_t versus t (Figure 9).

From Table 1 it is observed that the pseudo-second-order kinetic equation showed high correlation coefficients ($R^2 > 0.999$) for all three concentrations of aniline. In addition,

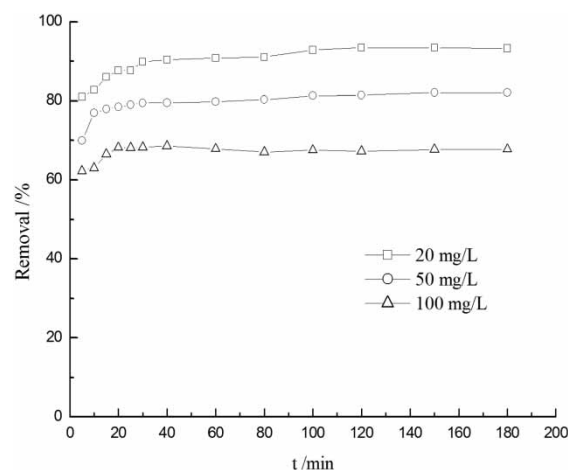


Figure 8 | Effect of contact time on aniline adsorption.

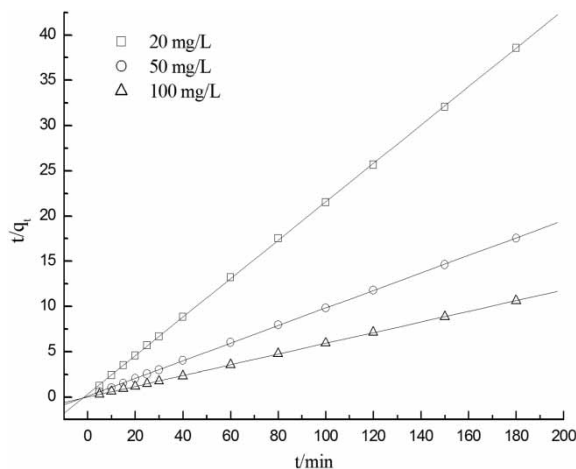


Figure 9 | Pseudo-second-order kinetic model for aniline adsorption.

Table 1 | Pseudo-second-order parameters of aniline adsorption onto AC coated by chitosan

Parameters (mg/L)	q_e (exp)	k_2	q_e (cal)	R^2
20	4.520	0.138	4.708	1.0000
50	9.815	0.268	10.246	0.9996
100	17.144	0.408	16.929	1.0000

the calculated q_e from the pseudo-second-order kinetic model was closely similar to the experimental q_e for aniline adsorption by AC coated by chitosan. Therefore, the pseudo-second-order kinetic model may be applied to predict the kinetic behavior of aniline adsorption. Besides, the values of the pseudo-second-order rate constant (k_2) were calculated as 0.138 mg/(g·min), 0.268 mg/(g·min) and 0.408 mg/(g·min) at the three selected concentrations: 20 mg/L, 50 mg/L and 100 mg/L, respectively. As observed, the k_2 value for aniline adsorption by AC coated by chitosan increased with increasing aniline concentrations. An increase in k_2 value indicated an increase in adsorption rate, and thus the equilibrium time was shortened. This result was in accordance with the phenomena mentioned previously in this section.

Adsorption isotherm

The adsorption isotherm models of Langmuir (Gao et al. 2009) and Freundlich (Barka et al. 2010) are usually used to describe the relationship between the adsorbent and

adsorbate. The Langmuir isotherm model assumes a saturated molecular layer (monolayer) on the adsorbent surface, while the Freundlich isotherm model assumes a heterogeneous surface and a multilayer adsorption with an energetic nonuniform distribution.

The Langmuir isotherm model can be expressed in Equation (4):

$$\frac{C_e}{q_e} = \frac{1}{Qb} + \frac{C_e}{Q} \quad (4)$$

where C_e (mg/L) is the equilibrium concentration of aniline in solution, q_e (mg/g) is the equilibrium adsorption capacity, Q (mg/g) is the maximum adsorption capacity per gram of sorbent, and b (L/mg) is the Langmuir constant related to the energy of adsorption. In this model, the dimensionless constant separation factor for the equilibrium parameter (R_L) can be defined as follows:

$$R_L = \frac{1}{1 + bC_0} \quad (5)$$

where C_0 (mg/L) is the initial concentration of aniline and b (L/mg) is the Langmuir constant. If the R_L value is between 0 and 1, the adsorption process is favorable.

The Freundlich isotherm model is presented in Equation (6):

$$\log q_e = \log K_f + \frac{1}{n} \log C_e \quad (6)$$

where C_e (mg/L) is the equilibrium concentration of aniline in solution, q_e (mg/g) is the equilibrium adsorption capacity, K_f (mg/g) and n are Freundlich constants related to adsorption capacity and the heterogeneity factor, respectively.

Linearized forms of Langmuir and Freundlich isotherms for the adsorption of aniline onto AC coated by chitosan are shown in Figures 10 and 11. The Q , b and R_L values for the Langmuir isotherm, the K_f and $1/n$ values for the Freundlich isotherm and the correlation coefficients of equations are shown in Table 2. Results show that the Freundlich equation gave a better fit than the Langmuir equation according to their correlation coefficients. The Langmuir isotherm equation did not better fit the experimental data, probably due to the heterogeneous distribution of active sites on the surface of the adsorbent tested. The R_L values lying between 0 and 1 indicated favorable conditions for the adsorption of

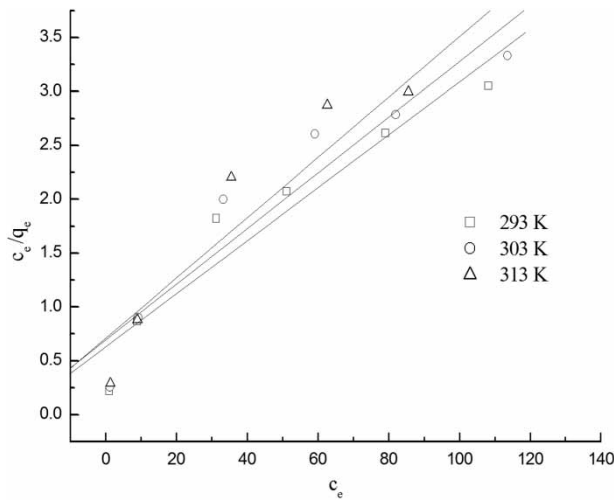


Figure 10 | Langmuir isotherm plots for aniline adsorption.

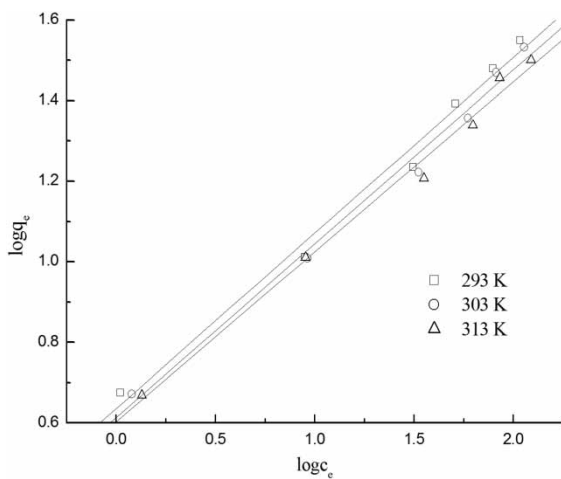


Figure 11 | Freundlich isotherm plots for aniline adsorption.

Table 2 | Langmuir and Freundlich isotherm parameters of aniline adsorption onto the adsorbent

Isotherms	Parameters	293K	303K	313K
Langmuir isotherm	Q	40.65	38.67	35.71
	b	0.039	0.037	0.040
	R_L	0.093–0.561	0.097–0.572	0.092–0.558
	R^2	0.9586	0.9521	0.9610
Freundlich isotherm	K_f	0.011	0.007	0.006
	n	2.295	2.318	2.372
	1/n	0.436	0.431	0.422
	R^2	0.9941	0.9944	0.9952

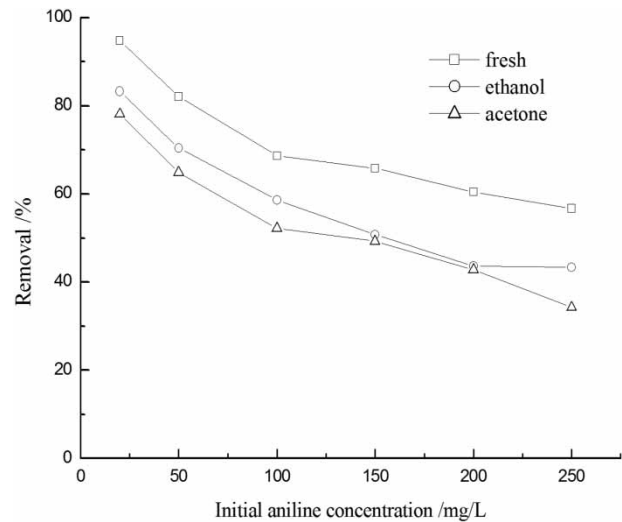


Figure 12 | Regeneration of AC by chitosan on aniline adsorption.

aniline onto AC coated by chitosan at all the temperatures studied. Further, for these adsorption processes, n values have been found to vary between 2.295 and 2.372, justifying the adsorption of aniline by AC coated by chitosan as a favorable process.

Desorption and regeneration

Desorption studies will help to regenerate the particles so that they can be reused to adsorb aniline. All the regeneration experiments were carried out at 20 °C. The desorption efficiency of the adsorbent was checked with organic solvents like ethanol and acetone. The results (Figure 12) show that ethanol is a better eluent compared with acetone. However, the two eluents, ethanol and acetone, seemed not to be the effective eluent.

CONCLUSIONS

FTIR analysis confirmed that AC was successfully coated by chitosan. The combination of AC and chitosan enhanced the adsorption of aniline as compared with chitosan alone. A reduced quantity of AC will be needed in the adsorption process using the composite of AC with chitosan. The adsorption of aniline onto AC coated by chitosan as a function of adsorbent dosage, initial aniline concentration, pH

value of aniline solution, and contact time was investigated by using batch experiments. The removal toward aniline decreased with increasing aniline concentration, while it increased with increasing adsorbent dosage. This adsorbent allowed high removal toward aniline across a wide range of pH values. The adsorption of aniline followed the pseudo-second-order equation. The adsorption isotherm of aniline can be well described by the Freundlich equation.

ACKNOWLEDGEMENT

This work was supported by the National Natural Science Foundation of China (Grant No. 51003086).

REFERENCES

- Al-Johani, H. & Salam, M. A. 2011 Kinetics and thermodynamic study of aniline adsorption by multi-walled carbon nanotubes from aqueous solution. *J. Colloid Interface Sci.* **360** (2), 760–767.
- An, F., Feng, X. & Gao, B. 2009 Adsorption of aniline from aqueous solution using novel adsorbent PAM/SiO₂. *Chem. Eng. J.* **151** (1), 183–187.
- Barka, N., Assabbane, A., Nounah, A., Laanab, L. & Ichou, Y. A. 2010 Removal of textile dyes from aqueous solutions by natural phosphate as a new adsorbent. *Desalination* **235** (1), 264–275.
- Chandra, V., Park, J., Chun, Y., Lee, J. W. & Hwang, I. C. 2010 Water-dispersible magnetite-reduced graphene oxide composites for arsenic removal. *ACS Nano* **4** (7), 3979–3986.
- Chang, Y. P., Ren, C. L., Qu, J. C. & Chen, X. G. 2012 Preparation and characterization of Fe₃O₄/graphene nanocomposite and investigation of its adsorption performance for aniline and *p*-chloroaniline. *Appl. Surf. Sci.* **261**, 504–509.
- Chu, W., Choy, W. K. & So, T. Y. 2007 The effect of solution pH and peroxide in the TiO₂-induced photocatalysis of chlorinated aniline. *J. Hazard. Mater.* **141** (1), 86–91.
- Crini, G. & Badot, P. M. 2008 Application of chitosan, a natural aminopolysaccharide, for dye removal from aqueous solutions by adsorption processes using batch studies: a review of recent literature. *Prog. Polym. Sci.* **33** (4), 399–447.
- Gao, S., Sun, R., Wei, Z. G., Zhao, H. Y. & Li, H. X. 2009 Size-dependent defluoridation properties of synthetic hydroxyapatite. *J. Fluorine Chem.* **130** (6), 550–556.
- Gupta, N., Kushwaha, A. K. & Chattopadhyaya, M. C. 2012 Adsorptive removal of Pb²⁺, Co²⁺ and Ni²⁺ by hydroxyapatite/chitosan composite from aqueous solution. *J. Taiwan Inst. Chem. Eng.* **43** (1), 125–131.
- Han, Y., Quan, X., Chen, S., Zhao, H., Cui, C. & Zhao, Y. 2006 Electrochemically enhanced adsorption of aniline on activated carbon fibers. *Sep. Purif. Technol.* **50** (3), 365–372.
- Hu, J., Huang, L. Y., Li, B. J., Zhang, W. & Ying, W. C. 2013 Granular activated carbon adsorption process for removing methyl tert-butyl ether from groundwater. *Asian J. Chem.* **25** (5), 2631–2636.
- Hydari, S., Shariffard, H., Nabavinia, M. & Parvizi, M. 2012 A comparative investigation on removal performances of commercial activated carbon, chitosan biosorbent and chitosan/activated carbon composite for cadmium. *Chem. Eng. J.* **193–194**, 276–282.
- Liu, X. & Zhang, L. 2015 Removal of phosphate anions using the modified chitosan beads: adsorption kinetic, isotherm and mechanism studies. *Powder Technol.* **277**, 112–119.
- Liu, T. Y., Wang, Z. L., Zhao, L. & Yang, X. 2012 Enhanced chitosan/Fe⁰-nanoparticles beads for hexavalent chromium removal from wastewater. *Chem. Eng. J.* **189–190**, 196–202.
- Ma, Y., Gao, N. Y., Chu, W. H. & Li, C. 2013 Removal of phenol by powdered activated carbon adsorption. *Front. Environ. Sci. Eng.* **7** (2), 158–165.
- Sapurina, I. Y. & Stejskal, J. 2012 Oxidation of aniline with strong and weak oxidants. *Russ. J. Gen. Chem.* **82** (2), 256–275.
- Viswanathan, N., Sundaram, C. S. & Meenakshi, S. 2009 Sorption behaviour of fluoride on carboxylated cross-linked chitosan beads. *Colloids Surf. B* **68** (1), 48–54.
- Wang, D., Zheng, G., Wang, S., Zhang, D. & Zhou, L. 2011 Biodegradation of aniline by candida tropicalis AN1 isolated from aerobic granular sludge. *J. Environ. Sci. Chin.* **23** (12), 2063–2068.
- Xie, Y., Li, S., Liu, G., Wang, J. & Wu, K. 2012 Equilibrium, kinetic and thermodynamic studies on perchlorate adsorption by cross-linked quaternary chitosan. *Chem. Eng. J.* **192**, 269–275.
- Xiong, J. B., Qin, Y., Islam, E., Yue, M. & Wang, W. F. 2011 Phosphate removal from solution using powdered freshwater mussel shells. *Desalination* **276** (1), 317–321.
- Xu, X., Song, W., Huang, D., Gao, B., Sun, Y., Yue, Q. & Fu, K. 2015 Performance of novel biopolymer-based activated carbon and resin on phosphate elimination from stream. *Colloid. Surface A* **476**, 68–75.
- Yakout, S. M., Daifullah, A. A. M. & El-Reefy, S. A. 2013 Adsorption of naphthalene, phenanthrene and pyrene from aqueous solution using low-cost activated carbon derived from agricultural wastes. *Adsorp. Sci. Technol.* **31** (4), 293–302.

First received 12 July 2014; accepted in revised form 28 April 2015. Available online 15 June 2015